IEEE Access
Multidisciplinary | Rapid Review | Open Access Journal

Received 25 August 2024, accepted 17 September 2024, date of publication 24 September 2024,
date of current version 14 October 2024.

Digital Object Identifier 10.1109/ACCESS.2024.3466993

APPLIED RESEARCH

Design of a Wideband High-Gain Monopulse Antenna for X- and Ku-Bands Applications

ZHI XING CHEN[1,2], ALI FARAHBAKHSH[3,4], JIA XIN LV[1], HUAFENG SU[1,5], AND XIU YIN ZHANG[1,5], (Fellow, IEEE)

[1]School of Electronic and Information Engineering, South China University of Technology, Guangzhou 510641, China
[2]Fuyao Glass Industry Group Company Ltd., Fuzhou 350300, China
[3]Electrical and Computer Engineering Department, Graduate University of Advanced Technology, Kerman 7631885356, Iran
[4]Department of Microwave and Antenna Engineering, Faculty of Electronics, Telecommunications, and Informatics, Gdańsk University of Technology, 80-233 Gdańsk, Poland
[5]Pazhou Laboratory, Guangzhou 510330, China

Corresponding author: Xiu Yin Zhang (zhangxiuyin@scut.edu.cn)

This work was supported by the National Natural Science Foundation of China under Grant 62031016.

ABSTRACT The present study provides a wideband high-gain monopulse antenna based on a dielectric lens operating in X- and Ku-bands, in which a wideband dielectric lens is designed and employed to fulfill the radiation pattern and bandwidth necessities of a monopulse antenna. The proposed configuration has four horns allowing for the simultaneous creation of Δ and Σ designs in two perpendicular planes. The main advantages of the proposed dielectric lens are low cost, lightweight, and easy fabrication using 3-D printing technology. The measurement findings show that the peak gain of the sum pattern is 28.9 dBi with a peak aperture efficiency of 60% over the desired frequency bandwidth. The suggested design can produce a simultaneous sum and two distinct difference patterns in orthogonal planes, meeting the rigorous demands for speed and accuracy in tracking applications.

INDEX TERMS Monopulse antenna, dielectric lens, wideband antenna.

I. INTRODUCTION

Monopulse radars mostly utilize tracking systems for various space and military uses, such as air traffic control, detection of cosmic debris, and satellite tracking [1]. The monopulse technique can withstand variations in target echo amplitudes and their reduced susceptibility to countermeasure systems, resulting in its wide use in precision tracking. The most straightforward conventional monopulse tracking feed system includes a feed with 4 or 5 antennas and a comparator network. Typically, such systems work independently at Ku-band (12-18 GHz) or X-band (8-12 GHz). Their sizes are bulky and not suitable for on-board tracking systems. As a result, a wideband antenna (covers the X- and Ku-band) and a simpler feed system to determine the orientation error [2] are more suitable for the monopulse radar.

Moreover, high-gain antennas are vital components of monopulse radars to increase signal coverage. Many monopulse systems, like point-to-point terrestrial links, deep space communication links, remote sensing systems, satellite communication links, and radars, require high-gain antennas to enhance signal coverage. The printed arrays [3], [4], [5], [6], [7], [8], [9], [10], [11], [12] are the common monopulse antennas with high gain. However, the array antenna demands a complex feeding system, leading to a complex antenna structure. The transmitarray/reflectarray [13], [14], [15], [16], [17], [18], [19], slot antennas [20], [21], [22], [23], [24], and metasurfaces [25], [26], [27] can be used to realize the high-gain monopulse antenna with a simpler feed system. However, the bandwidth of a monopulse antenna is relatively narrow considering the resonant structures like periodic unit cells and slots generally used in most structures. Reference [20] discusses the implementation of a radial line slot monopulse antenna with a 5.86 cm radius, achieving broadside directivity of 23 dBi and 4.4% relative bandwidth in the Ku-band. A 16 $\times$ 16 circularly polarized W-band monopulse antenna array with 8.5% impedance bandwidth and gain of 32.2 dBi was proposed in [22]. In [23], an affordable and

The associate editor coordinating the review of this manuscript and approving it for publication was Hassan Tariq Chattha.

compact radial line slot monopulse antenna with a diameter of 4.5 cm for aperture, designed to operate at 94 GHz with directivity of 32.3 dBi and 8.5% impedance bandwidth. In [24], a gap waveguide technology-based monopulse antenna with 3 layers was proposed to achieve gain of 27 dBi from 29 to 31 GHz. The authors of [26] suggest the synthesis of difference and sum beams according to a binary programmable metasurface at 28 GHz to obtain gain of 21.34 dBi. Also, reference [27] proposed a metasurface-based monopulse antenna with a 15-cm diameter, realizing the sum gain of 28 dBi and 10% relative bandwidth. Narrow frequency bandwidth is the major drawback of most proposed structures.

The use of multimode antennas has also been considered to achieve narrowband monopulse performance [28], [29], [30], [31]. For example, a multimode horn feed with a monopulse performance operating at 35 GHz and a bandwidth of 2.3% was presented in [30]. In addition to the aforementioned methods, dielectric-lens antennas have also been used to design high-gain monopulse antennas [32], [33], [34], [35]. For instance, the authors of [34] suggest the design of a narrowband monopulse antenna according to a dielectric lens at 94 GHz. In [35], a dielectric lens-based monopulse antenna was proposed to realize the gain of 32.3 dBi and 12% relative bandwidth at 35 GHz. All of these structures suffer from narrow frequency bandwidth.

To our knowledge, a wideband monopulse antenna using a dielectric lens with an almost fixed phase center and high gain has not been introduced yet. In this respect, no similar monopulse antenna has been presented in the literature in the 8-18 GHz frequency range and with a monopulse gain of 28.9 dBi. In this contribution, this paper deals with designing a monopulse antenna based on a dielectric lens, featuring a simple feed system, wideband, and high-gain antenna performance to cover X- and Ku-bands.

The remainder of this paper is structured as follows: Section II deals with designing dielectric lenses. The development of a dielectric lens with multiple feeds is discussed in Section III. Section IV is devoted to the empirical validation of the presented designs. Finally, a table is provided to indicate the performance enhancement of the developed monopulse antenna compared to other studies.

II. DESIGN OF HORN ANTENNA AND DIELECTRIC LENS

A. DIELECTRIC LENS

In recent years, dielectric lenses have extensively been studied for their benefits, including simple structure, easy manufacturing using 3D printing methods, low cost, lightweight, and high transmission coefficient [36], [37], [38]. The proposed configuration of the three-dimensional dielectric lens is shown in Fig. 1. For simple fabrication, the proposed lens is considered a multilayered cylindrical structure. The dielectric constant of the employed material is 2.08. The proposed structure has 10 rings with different heights and the same width of W_R.

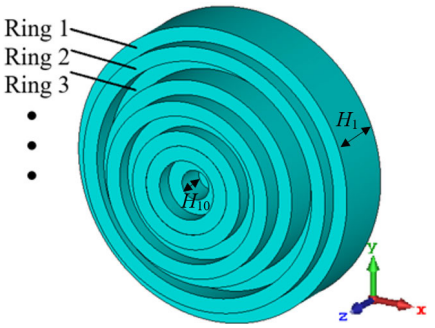

FIGURE 1. Configuration of the proposed dielectric lens consists of 10 cylindrical rings with the same width and different heights ($H_1 \sim H_{10}$).

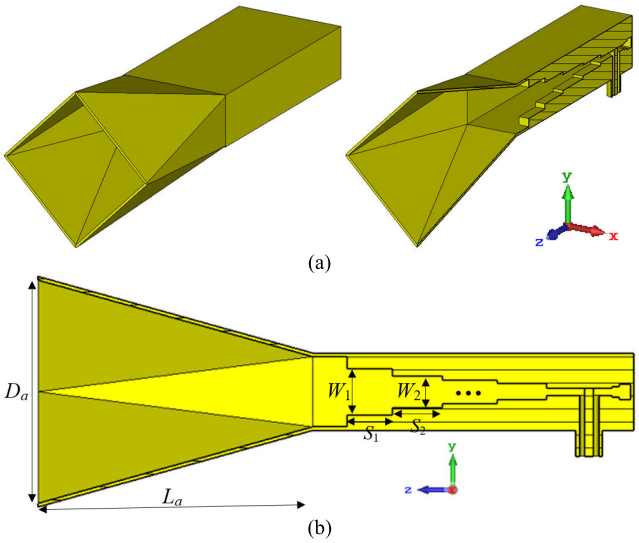

FIGURE 2. Configuration of a typical diagonal horn antenna. (a) Perspective view. (b) Side view. The geometrical parameters (in mm) are $D_a = 32.33$, $L_a = 40$, $W_1 = 6.67$, $W_2 = 6.44$, $W_3 = 3.42$, $W_4 = 2.35$, $W_5 = 1.09$, $W_6 = 1.51$, $W_7 = 2.29$, $S_1 = 6.61$, $S_2 = 7.24$, $S_3 = 8.00$, $S_4 = 7.16$, $S_5 = 9.52$, $S_6 = 1.16$, $S_7 = 1.58$.

The height of the rings ($H_1 \sim H_{10}$) and their width should be selected through the optimization approach such that in the desired frequency range from 8 to 18 GHz, the preferred radiation pattern with maximum gain is obtained, and the designed lens has an almost constant phase center or with minimal displacement rather than center feed of a broadband horn antenna.

B. Horn Antenna Design

In this design, a diagonal horn antenna feeds the lens. Fig. 2 illustrates the antenna's structure and its dimensions. The wideband transition from coaxial to WR-90 rectangular waveguide used in this design is designed with multiple steps, and it has a standard SMA connector with a probe diameter of 1.25 mm. Like the corrugated horn antenna, the diagonal horn antenna has a nearly symmetrical radiation beam around the antenna axis. It is of note that the structure of this type of antenna is much simpler and less expensive than the corrugated horn antenna. In many monopulse systems, it is

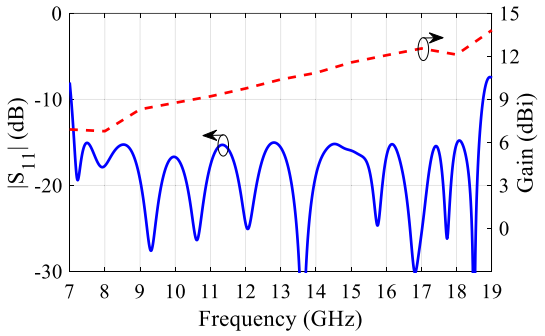

FIGURE 3. Simulation results for the $|S_{11}|$ and gain of the diagonal horn antenna.

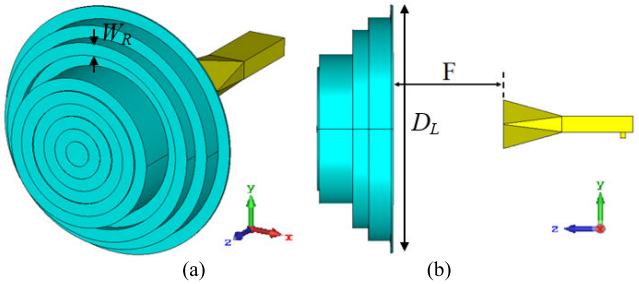

FIGURE 4. Configuration of the proposed lens antenna. (a) front view, (b) side view.

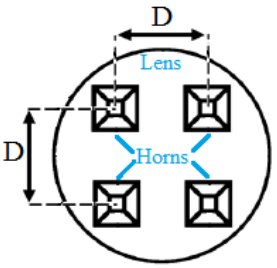

FIGURE 5. Quad-feed configurations for dielectric lens antenna.

necessary to access horizontal, vertical, and 45° slant polarization. With the characteristic of symmetry in the radiation beam of the diagonal horn antenna, the desired polarization can be achieved simply by rotating each of these antennas.

The design is validated by conducting electromagnetic simulations using a time domain solver within the CST Microwave Studio. These simulations model the conducting components as being made of Aluminum with an electrical conductivity of 3.6×10^7 S/m. The horn antenna's aperture size is 22.86 × 22.86 mm and the width of the multistep ridge section is 4.51 mm. Fig. 3 demonstrates the simulated reflection coefficient and realized gains of the diagonal horn antenna against frequency. Note that the $|S_{11}|$ of the antenna is under −10 dB from 7 to 18.75 GHz with a peak gain of 12.8 dBi.

C. COMPLETE LENS ANTENNA

The preferred radiation pattern of the general structure of the lens antenna can be achieved by placing the proposed horn feed in front of the lens. The phase centers of the feeding horn

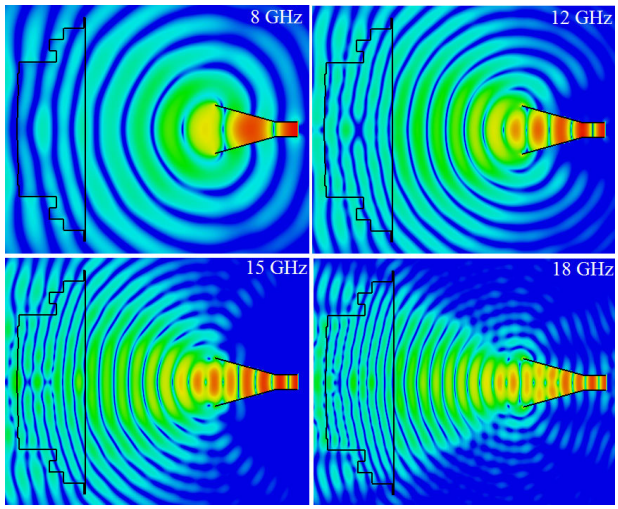

FIGURE 6. Electric field distribution of the lens antennas at different frequencies.

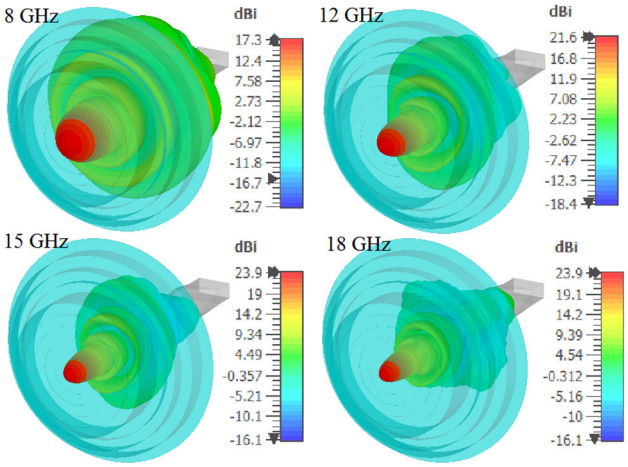

FIGURE 7. 3D radiation patterns of the lens antennas at different frequencies.

antenna and the lens should coincide as much as possible in the desired frequency range to achieve a high gain antenna. To realize the design goals, optimization is done using the Trust Region Framework optimization technique to meet the design criteria. The design parameters are ($H_1 \sim H_{10}$), W_R *and* F. The initial values for these design parameters are $2\lambda_0$, $\lambda_0/4$ and $2\lambda_0$, respectively, wherein $\lambda_0$is the free space wavelength in center frequency (13 GHz). The allowable ranges of the design parameter in the optimization are assumed to be 1∼50, 5∼10 and 30∼60 (in mm), respectively.

Fig. 4 represents the configuration of the complete lens antenna. In this structure, 10 rings with a width of $W_R = 7.5$ mm form a lens with a diameter of $D_L = 15$ cm. The heights of rings ($H_1 \sim H_{10}$) are 1.03, 14.44, 24.05, 19.29, 44.16, 45.21, 44.76, 45.15, 45.34 and 45.52 mm, respectively. The optimized value for the distance between the lens and antenna is $F = 50$ mm. Fig. 5 illustrates the structure's electric field distribution at 13 GHz. As can be seen, it is possible to focus the fields on about the same region, and the spherical

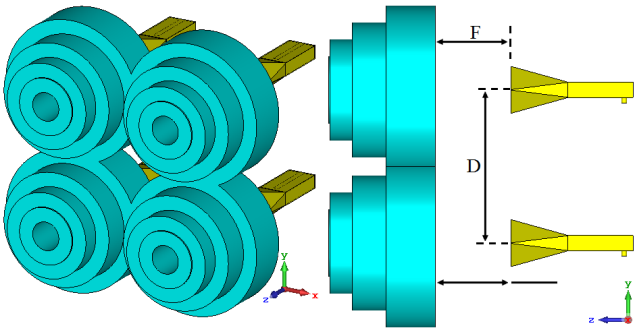

FIGURE 8. Configurations of monopulse dielectric lens antenna.

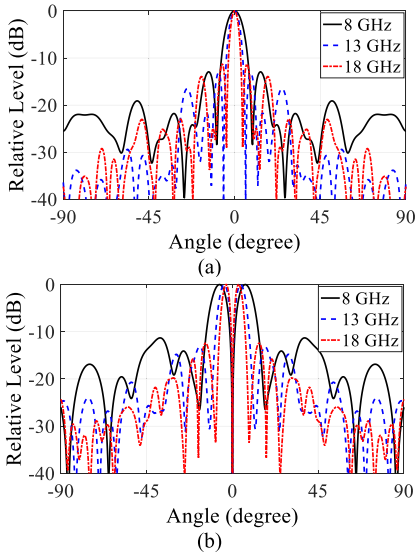

FIGURE 9. Simulated normalized radiation patterns of dielectric lens antenna. (a) Sum mode. (b) Difference Mode.

wave radiated from the focus is transformed into a planar wave. Thus, the high-gain beams are formed, as shown in Fig. 6. The effect of the dielectric lens on the performance of the diagonal horn antenna can be summarized in increasing the gain and improving the characteristics of the radiation pattern. According to Figs. 3 and 6, the maximum gain of the horn antenna by placing the lens in front of it has reached from about 13.5 dBi to about 23.9 dBi at the frequency of 18 GHz. Eventually, a wideband high-gain monopulse antenna with a one-horn feed system is obtained.

III. DIELECTRIC LENS WITH MULTIPLE FEEDS

After proving the presented concept and ensuring the proper performance of the single-fed dielectric lens antenna, a structure is proposed to achieve monopulse performance. As can be noticed, when 4 antennas are placed instead of a horn antenna and the design goal is achieving the preferred properties of sum and difference modes, the antennas' mutual coupling and their distance affect factors that are not considered in single-fed antenna. Therefore, the dimensions and shape of the monopulse lens antenna are expected to be different from a single-feed lens antenna. The representation

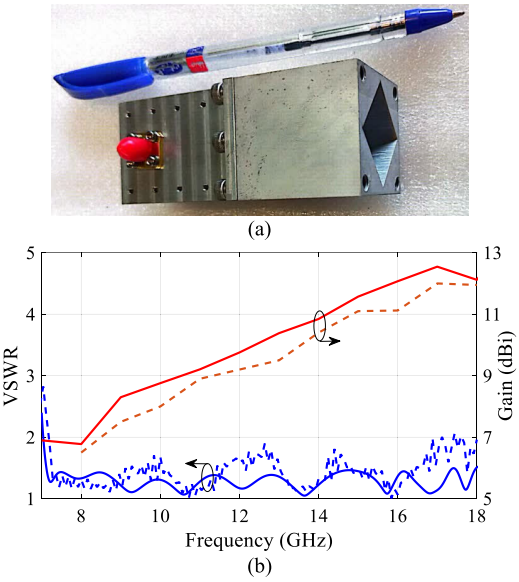

FIGURE 10. Photographs of (a) fabricated horn prototype antenna, (b) Simulated (solid) and measured (dashed) VSWR and gain of the diagonal horn antenna.

of the suggested configuration is illustrated in Fig. 7. In this structure, a dielectric lens is illuminated by four horns located at the *F*distance from the lens. Fig. 8 shows that the presented dielectric lens contains four lenses consisting of five rings placed together and overlapping. Such a structure is considered for its small size and simplicity of construction. The research in [41] was conducted for two configurations: dual-feed and quadruple-feed transmitarrays. Investigation of impact of the *D*and *F* on the gain of the multiple-fed transmit arrays showed that employing a quadruple-feed system lowers the focal length by approximately half while maintaining radiation characteristics similar to those of a single-feed transmit array.

It is necessary to specify the geometrical parameters of the structure for creating a suitable monopulse performance across a specific frequency bandwidth from 8 to 18 GHz. In the proposed configuration, the three parameters F, d, and D, and the heights of rings ($H_1 \sim H_5$) should be determined and optimized to reach acceptable antenna characteristics in both sum and differential modes. It is important to highlight that achieving excellent performance requires optimal values for the geometric parameters of the structure in the sum mode, which are not necessarily appropriate for the difference mode. In other words, the optimized structure for the sum mode will not be appropriate for the difference mode. This challenge is solved using CST Microwave Studio's simultaneous combined optimization tools. Optimization is done using the Trust Region Framework optimization technique to meet the design criteria. The final optimized values for the width of each ring, D, and F are 12, 109.32, and 54.21 mm, respectively. Also, the optimized heights of the rings ($H_1 \sim H_5$) are 35.17, 59.12, 74.80, 76.06, and 27.48 mm, respectively.

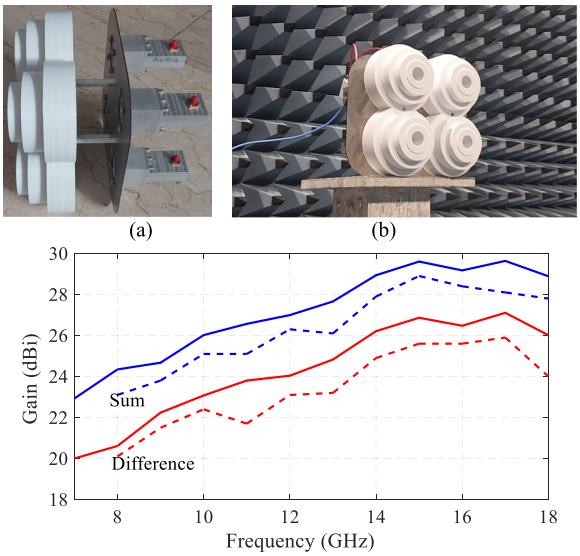

FIGURE 11. (a) complete dielectric lens antenna and (b) under test antenna. (c) Simulated (solid) and measured (dashed) gain of dielectric lens antenna in sum and difference modes. The measured values are illustrated with dashed lines.

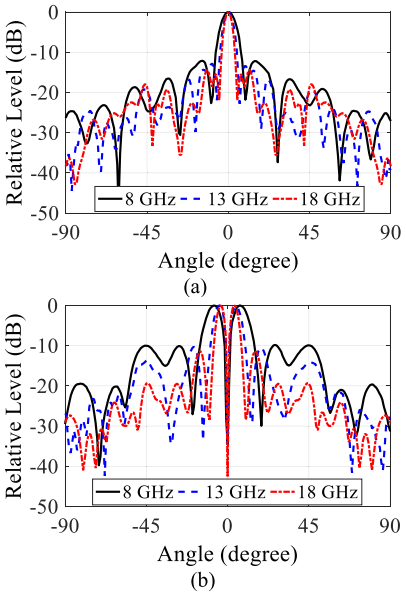

FIGURE 12. Measured normalized radiation patterns of dielectric lens antenna. (a) Sum mode. (b) Difference Mode.

Fig. 9 depicts the normalized radiation patterns of the antenna at 8, 12, and 18 GHz, showing antenna radiation at the sum and difference modes. As can be seen, the null depth is below −40 dB in the difference patterns.

IV. FABRICATION AND MEASUREMENT

The horn antenna prototype fabricated in low-loss AA6061 aluminum by standard milling approaches (Fig. 10(a)) was used to validate the presented designs. Measurements were performed using the Agilent N5230 vector network analyzer. The comparison of measured VSWR and gain of the diagonal horn antenna versus frequency with simulation results are presented in Fig. 10(b). As can be seen, the calculated

TABLE 1. Antennas performances comparison with previously reported similar antennas.

Ref.	Type	Band	B.W (%)	Gain (dBi)	Null Depth (dB)	Efficiency (%)	Size (λ_0^2)
[4]	Microstrip	Ku	5.6	24.5	-30	20	13.3×12.3
[5]	Microstrip	Ku	28.2	18.4	-28	-	4.1×4.1
[7]	SIW	Ka	7.4	18.7	-46.3	3.9	14.5×10.4
[8]	SIW	W	1.6	25.8	-45.8	15.2	41×39.4
[10]	SIW	X	4	9.5	-22	21	4.1×0.8
[15]	SIW	X	3	16.4	-33.8	43	3.9×2
[14]	Transmitarray	Ka	15	23.2	-22.7	50	-
[16]	Reflectarray	Ka	3	29.4	-30	22.4	19.8×19.8
[19]	Transmitarray	X	4	21.5	-18.6	32.2	6.7×6.7
[20]	Slot Array	Ku	4.4	22.2	-25	58.7	6.4×6.4
[23]	Gap Waveguide	W	0.83	27.8	-40	70	47×18.8
[27]	Metasurface	Ka	13	28	-22	42	16.7×16.7
[32]	Dielectric Lens	W	1	35	-42	NA	NA
[33]	Dielectric Lens	Ka	16.2	12	-20	NA	7.6×7.6
[35]	Dielectric Lens	Ka	12	32.3	-30	50	16×16
This Work	Dielectric Lens	X & Ku	86	28.9	-40	60	10×10

frequency VSWR<2 is from 7.15 GHz to 18 GHz, corresponding to 86% impedance bandwidth. The suggested horn antenna presents a gain of 6.8-12.8 dBi in the specified frequency range.

Figs. 11(a) and 11(b) represent the fabricated dielectric lens antenna. In [39] and [40], the design of a dielectric lens and its fabrication using 3D-printing is discussed in detail. Briefly, it provides a practical and low-cost method to fabricate a dielectric lens with different relative permittivity from 1.30 to 2.72. Here, 3-D printing was performed by using 58% infilled thermoplastic polylactic acid with a relative permittivity of 2.08 and a loss tangent of 0.008.

The antenna's radiation patterns are assessed using an anechoic chamber measurement system. Fig. 11(c) compares the measured and simulated realized antenna gains in the sum and difference modes across various frequencies. The measurements indicate that the antenna's gain in the sum mode is approximately 3 dB higher than in the difference mode. The presented antenna achieves a peak gain of 28.9 dBi over 8 to 18 GHz frequency range in the sum mode. The measured aperture efficiency falls between 43% and 60% within the 8-18 GHz band. A consistency was noted between the simulated and measured gain for the suggested antenna. The decrease of 0.5-1 dB of measured gain compared with the simulation values is assigned to additional losses resulting from factors such as metal conductivity degradation, higher dielectric loss, fabrication inaccuracies, and measurement setup errors.

Fig. 12 presents the antenna's simulated and measured radiation patterns at various frequencies in both the sum

and difference modes. There is a strong correlation between the measurement and simulation results, indicating that both manufactured antennas produce monopulse radiation patterns across the extensive operating bandwidth. Any variation in the results can be attributed to inherent inaccuracies in the pattern measurement setup. The sum and difference patterns show side lobe levels below -12.3 dB and -10 dB.

The performance of the developed monopulse antennas was assessed by comparing the measured specifications of the (Table 1). In microstrip- and SIW-based structures, where dielectric substrates are present, the antenna efficiency falls below 40%. However, in complete metal structures with no reflector elements, the antenna efficiency exceeds 70%. The results obtained for the proposed antenna demonstrate favorable characteristics, including well-behaved sum and difference patterns, a measured gain of nearly 29 dBi, an antenna peak efficiency of 60% for the sum beam, a deep null of −40 dB for the difference beam, and an effective fractional impedance bandwidth of about 86%. These findings outperform those of the compared works, indicating that the proposed antenna exhibits superior overall performance. This superiority is more noticeable concerning wide bandwidth, logical gain, and dimension features as the key considerations in wideband monopulse systems.

V. CONCLUSION

A wideband high-gain monopulse antenna was proposed empirically and numerically based on a 3D printed dielectric lens for X- and Ku-band applications. The proposed structures caused significant improvement in impedance bandwidth compared to conventional monopulse antennas. The fabricated dielectric lens monopulse antenna achieved a 2.52:1 ratio bandwidth from 7.15 to 18 GHz with a 29 dBi peak gain. The suggested wideband monopulse antenna has potential applications in various military, radar, and tracking scenarios.

REFERENCES

[1] M. Skolnik, *Introduction to Radar Systems*. New York, NY, USA: McGraw-Hill, 2001.

[2] S. M. Sherman and D. K. Barton, *Monopulse Principles and Techniques*. Norwood, MA, USA: Artech House, 1984.

[3] A. Lopez, "Monopulse networks for series feeding an array antenna," *IEEE Trans. Antennas Propag.*, vol. AP-16, no. 4, pp. 436–440, Jul. 1968.

[4] H. Wang, D.-G. Fang, and X. G. Chen, "A compact single layer monopulse microstrip antenna array," *IEEE Trans. Antennas Propag.*, vol. 54, no. 2, pp. 503–509, Feb. 2006.

[5] Z.-W. Yu, G.-M. Wang, and C.-X. Zhang, "A broadband planar monopulse antenna array of C-band," *IEEE Antennas Wireless Propag. Lett.*, vol. 8, pp. 1325–1328, 2009.

[6] H. Wang, D.-G. Fang, and M. Li, "A single-channel microstrip electronic tracking antenna array with time sequence phase weighting on sub-array," *IEEE Trans. Microw. Theory Techn.*, vol. 58, no. 2, pp. 253–258, Feb. 2010.

[7] B. Liu, W. Hong, Z. Kuai, X. Yin, G. Luo, J. Chen, H. Tang, and K. Wu, "Substrate integrated waveguide (SIW) monopulse slot antenna array," *IEEE Trans. Antennas Propag.*, vol. 57, no. 1, pp. 275–279, Jan. 2009.

[8] Y. J. Cheng, W. Hong, and K. Wu, "94 GHz substrate integrated monopulse antenna array," *IEEE Trans. Antennas Propag.*, vol. 60, no. 1, pp. 121–129, Jan. 2012.

[9] K. Tekkouk, M. Ettorre, L. Le Coq, and R. Sauleau, "SIW pillbox antenna for monopulse radar applications," *IEEE Trans. Antennas Propag.*, vol. 63, no. 9, pp. 3918–3927, Sep. 2015.

[10] J. Soleiman Meiguni, S. A. Khatami, and A. Amn-e-Elahi, "Compact substrate integrated waveguide mono-pulse antenna array," *Int. J. RF Microw. Comput.-Aided Eng.*, vol. 28, no. 1, Jan. 2018, Art. no. e21155.

[11] W. Li, S. Liu, J. Deng, Z. Hu, and Z. Zhou, "A compact SIW monopulse antenna array based on microstrip feed," *IEEE Antennas Wireless Propag. Lett.*, vol. 20, no. 1, pp. 93–97, Jan. 2021.

[12] Y. Cao and S. Yan, "A dual-mode SIW compact monopulse comparator for sum and difference multibeam radar applications," *IEEE Microw. Wireless Compon. Lett.*, vol. 32, no. 1, pp. 41–44, Jan. 2022.

[13] W. Hu, M. Y. Ismail, R. Cahill, J. A. Encinar, V. F. Fusco, H. S. Gamble, D. Linton, R. Dickie, N. Grant, and S. P. Rea, "Liquid-crystal-based reflectarray antenna with electronically switchable monopulse patterns," *Electron. Lett.*, vol. 43, no. 14, p. 744, 2007.

[14] L. Di Palma, A. Clemente, L. Dussopt, R. Sauleau, P. Potier, and P. Pouliguen, "Radiation pattern synthesis for monopulse radar applications with a reconfigurable transmitarray antenna," *IEEE Trans. Antennas Propag.*, vol. 64, no. 9, pp. 4148–4154, Sep. 2016.

[15] X. Pan, F. Yang, S. Xu, and M. Li, "An X-band reconfigurable reflectarray antenna with steerable monopulse patterns," in *Proc. Int. Appl. Comput. Electromagn. Soc. Symp.-China (ACES)*, Beijing, China, Jul. 2018, pp. 1–2.

[16] J. Zhao, H. Li, X. Yang, W. Mao, B. Hu, T. Li, H. Wang, Y. Zhou, and Q. Liu, "A compact Ka-band monopulse Cassegrain antenna based on reflectarray elements," *IEEE Antennas Wireless Propag. Lett.*, vol. 17, no. 2, pp. 193–196, Feb. 2018.

[17] X. Pan, F. Yang, S. Xu, and M. Li, "A 10 240-element reconfigurable reflectarray with fast steerable monopulse patterns," *IEEE Trans. Antennas Propag.*, vol. 69, no. 1, pp. 173–181, Jan. 2021.

[18] Y. Gao, W. Jiang, W. Hu, Q. Wang, W. Zhang, and S. Gong, "A dual-polarized 2-D monopulse antenna array for conical conformal applications," *IEEE Trans. Antennas Propag.*, vol. 69, no. 9, pp. 5479–5488, Sep. 2021.

[19] N. Kou, S. Yu, Z. Ding, and Z. Zhang, "Monopulse transmitarray antenna fed by aperture-coupled microstrip structure," *Frontiers Inf. Technol. Electron. Eng.*, vol. 23, no. 3, pp. 502–510, Mar. 2022.

[20] M. Sierra-Castaner, M. Sierra-Perez, M. Vera-Isasa, and J. L. Fernandez-Jambrina, "Low-cost monopulse radial line slot antenna," *IEEE Trans. Antennas Propag.*, vol. 51, no. 2, pp. 256–263, Feb. 2003.

[21] D. Comite, S. K. Podilchak, P. Baccarelli, P. Burghignoli, A. Galli, A. P. Freundorfer, and Y. M. M. Antar, "Design of a polarization-diverse planar leaky-wave antenna for broadside radiation," *IEEE Access*, vol. 7, pp. 28672–28683, 2019.

[22] E. Garcia-Marin, J.-L. Masa-Campos, and P. Sanchez-Olivares, "Diffusion-bonded W-band monopulse array antenna for space debris radar," *AEU-Int. J. Electron. Commun.*, vol. 116, Mar. 2020, Art. no. 153061.

[23] A. Tamayo-Domínguez, J.-M. Fernández-González, and M. Sierra-Castañer, "Monopulse radial line slot array antenna fed by a 3-D-printed cavity-ended modified Butler matrix based on gap waveguide at 94 GHz," *IEEE Trans. Antennas Propag.*, vol. 69, no. 8, pp. 4558–4568, Aug. 2021.

[24] M. Ferrando-Rocher, J. I. Herranz-Herruzo, A. Valero-Nogueira, and B. Bernardo-Clemente, "All-metal monopulse antenna array in the Ka-band with a comparator network combining ridge and groove gap waveguides," *IEEE Antennas Wireless Propag. Lett.*, vol. 22, no. 6, pp. 1381–1385, Jun. 2023.

[25] T. Li and Z. N. Chen, "Wideband substrate-integrated waveguide-fed end-fire metasurface antenna array," *IEEE Trans. Antennas Propag.*, vol. 66, no. 12, pp. 7032–7040, Dec. 2018.

[26] X. Wan, Q. Xiao, Y. Z. Zhang, Y. Li, J. Eisenbeis, J. W. Wang, Z. A. Huang, H. X. Liu, T. Zwick, and T. J. Cui, "Reconfigurable sum and difference beams based on a binary programmable metasurface," *IEEE Antennas Wireless Propag. Lett.*, vol. 20, no. 3, pp. 381–385, Mar. 2021.

[27] M. Faenzi, D. González-Ovejero, G. Petraglia, G. D'Alterio, F. Pascariello, R. Vitiello, and S. Maci, "A metasurface radar monopulse antenna," *IEEE Trans. Antennas Propag.*, vol. 70, no. 4, pp. 2571–2579, Apr. 2022.

[28] P. Hannan, "Optimum feeds for all three modes of a monopulse antenna II: Practice," *IRE Trans. Antennas Propag.*, vol. 9, no. 5, pp. 454–461, Sep. 1961.

[29] R. Shen, X. Ye, and J. Miao, "Design of a multimode feed horn applied in a tracking antenna," *IEEE Trans. Antennas Propag.*, vol. 65, no. 6, pp. 2779–2788, Jun. 2017.
[30] L. Polo-López, J. Córcoles, J. A. Ruiz-Cruz, J. R. Montejo-Garai, and J. M. Rebollar, "Triple-radiation pattern monopulse horn feed with compact single-layer comparator network," *IEEE Trans. Antennas Propag.*, vol. 69, no. 5, pp. 2546–2559, May 2021.
[31] Y. Chen, Y. Wang, H. Meng, and W. Dou, "W-band multimode monopulse horn feed for reflector antenna," *Microw. Opt. Technol. Lett.*, vol. 66, no. 2, Feb. 2024.
[32] S. Raman, N. S. Barker, and G. M. Rebeiz, "A W-band dielectric-lens-based integrated monopulse radar receiver," *IEEE Trans. Microw. Theory Techn.*, vol. 46, no. 12, pp. 2308–2316, Dec. 1998.
[33] L. Schulwitz and A. Mortazawi, "A monopulse Rotman lens phased array for enhanced angular resolution," in *IEEE MTT-S Int. Microw. Symp. Dig.*, Honolulu, HI, USA, Jun. 2007, pp. 1871–1874.
[34] Z. X. Wang and W. B. Dou, "Full-wave analysis of monopulse dielectric lens antennas at W-band," *J. Infr., Millim., Terahertz Waves*, vol. 31, pp. 151–161, Oct. 2010.
[35] A. Gorshkov, Q. Zhang, K.-H. Oh, J.-H. Kim, and B.-C. Ahn, "Design of a high-performance 35 GHz monopulse lens antenna," *J. Korean Inst. Inf. Technol.*, vol. 17, no. 3, pp. 79–86, Mar. 2019.
[36] N. C. Garcia and J. D. Chisum, "High-efficiency, wideband GRIN lenses with intrinsically matched unit cells," *IEEE Trans. Antennas Propag.*, vol. 68, no. 8, pp. 5965–5977, Aug. 2020.
[37] W. Yu, L. Peng, Y. Liu, Q. Zhao, X. Jiang, and S. Li, "An ultrawideband and high-aperture-efficiency all-dielectric lens antenna," *IEEE Antennas Wireless Propag. Lett.*, vol. 20, no. 12, pp. 2442–2446, Dec. 2021.
[38] A. Piroutiniya, M. H. Rasekhmanesh, J. L. Masa-Campos, J. López-Hernández, E. García-Marín, A. Tamayo-Domínguez, P. Sánchez-Olivares, and J. A. Ruiz-Cruz, "Beam steering 3D printed dielectric lens antennas for millimeter-wave and 5G applications," *Sensors*, vol. 23, no. 15, p. 6961, Aug. 2023.
[39] S. Zhang, Y. Vardaxoglou, W. Whittow, and R. Mittra, "3D-printed graded index lens for RF applications," in *Proc. Int. Symp. Antennas Propag. (ISAP)*, Okinawa, Japan, Oct. 2016, pp. 90–91.
[40] S. Zhang, R. K. Arya, S. Pandey, Y. Vardaxoglou, W. Whittow, and R. Mittra, "3D-printed planar graded index lenses," *IET Microw., Antennas Propag.*, vol. 10, no. 13, pp. 1411–1419, 2016.
[41] A. Clemente, L. Dussopt, R. Sauleau, P. Potier, and P. Pouliguen, "Focal distance reduction of transmit-array antennas using multiple feeds," *IEEE Antennas Wireless Propag. Lett.*, vol. 11, pp. 1311–1314, 2012.

ZHI XING CHEN is currently pursuing the Ph.D. degree with South China University of Technology currently. He is also the Director of the Intelligent Networking Department, Fuyao Group. He is mainly carry out research on antennas and passive components for various terminals and base stations, including microwave reflector antennas, array antennas, horn antennas, and microstrip antennas.

ALI FARAHBAKHSH was born in Kerman, Iran, in 1984. He received the Ph.D. degree in electrical engineering from Iran University of Science and Technology, Tehran, Iran, in 2016. He is currently an Associate Professor with the Department of Electrical and Computer Engineering, Graduate University of Advanced Technology, Kerman. He is also a Guest Associate Professor with Gdańsk University of Technology, Gdańsk, Poland, hosted by Prof. Michal Mrozowski. His research interests include microwave and antenna engineering, including gap waveguide technology, millimeter-wave high-gain array antenna, microwave devices, electromagnetic waves propagation and scattering, inverse problems in electromagnetic, and anechoic chamber design.

JIA XIN LV was born in Xingtai, Hebei, China. He received the B.S. degree from South China University of Technology, Guangzhou, China, in 2023, where he is currently pursuing the M.E. degree. His research interests include the filtering antennas, transparent antennas, and antenna arrays.

HUAFENG SU received the M.S. degree in communication engineering from Nanjing University, Nanjing, China, in 2016, and the Ph.D. degree in electromagnetic field and microwave technology from the South China University of Technology, Guangzhou, China, in 2023.

From 2005 to 2016, he was with COMMSCOPE Corporation, Shenzhen and Suzhou, China. From 2016 to 2019, he was the Director of the Antenna Department, NRADIO Corporation, Shenzhen, China. In 2019, he joined Gremtech, Shenzhen, as the Technical Director of the Research and Development Department. Currently, he is an Associate Research Fellow with the Pazhou Laboratory, Guangzhou.

XIU YIN ZHANG (Fellow, IEEE) received the B.S. degree in communication engineering from Chongqing University of Posts and Telecommunications, Chongqing, China, in 2001, the M.S. degree in electronic engineering from South China University of Technology, Guangzhou, China, in 2006, and the Ph.D. degree in electronic engineering from the City University of Hong Kong, Hong Kong, China, in 2009.

From 2001 to 2003, he was with ZTE Corporation, Shenzhen, China. He was a Research Assistant (July 2006–June 2007) and a Research Fellow (September 2009–February 2010) with the City University of Hong Kong. He is currently a Full Professor with the School of Electronic and Information Engineering, South China University of Technology. He has authored or co-authored more than 200 internationally refereed journal articles (including more than 130 IEEE TRANSACTIONS) and 100 conference papers. His research interests include antennas, RFIC, RF components and sub-systems, and intelligent wireless communications and sensing. He is a fellow of the Institution of Engineering and Technology (IET). He was a recipient of the National Science Foundation for Distinguished Young Scholars of China. He won the First Prize of the 2016 Guangdong Provincial Natural Science Award and the 2021 Guangdong Provincial Technological Invention Award. He was a supervisor of several conference best paper award winners. He serves as the Vice Chair for the IEEE Guangzhou Section and the Director of the Engineering Research Center of Short-Distance Wireless Communications and Network, Ministry of Education. He has served as the general chair/the co-chair/the technical program committee (TPC) chair/the co-chair of several conferences. He is or was an Associate Editor of IEEE TRANSACTIONS ON ANTENNAS AND PROPAGATION, IEEE ANTENNAS AND WIRELESS PROPAGATION LETTERS, *IEEE Antennas and Propagation Magazine*, and IEEE OPEN JOURNAL OF ANTENNAS AND PROPAGATION.